Journal of Organometallic Chemistry 694 (2009) 1081–1090

Contents lists available at ScienceDirect

Journal of Organometallic Chemistry

journal homepage: www.elsevier.com/locate/jorganchem

Ethylene addition to $Ru(=CH_2)(=O)_3$ – A theoretical study

Robin Haunschild [a], Sandor Tüllmann [b], Gernot Frenking [a,*], Max C. Holthausen [b,*]

[a] Fachbereich Chemie der Philipps-Universität Marburg, Hans-Meerwein-Straße, 35043 Marburg, Germany
[b] Institut für Anorganische Chemie der Johann Wolfgang Goethe-Universität, Max-von-Laue-Straße 7, D-60438 Frankfurt am Main, Germany

ARTICLE INFO

Article history:
Received 23 July 2008
Received in revised form 8 October 2008
Accepted 10 October 2008
Available online 17 October 2008

Keywords:
Oxidation reactions
Reaction mechanisms
Quantum chemical calculations
Ruthenium compounds
Carbenes

ABSTRACT

Quantum chemical calculations using density functional theory (B3LYP) were carried out to elucidate the reaction pathways for ethylene addition to the ruthenium compound RuO_3CH_2. These investigations show that the parent compound is relatively unstable and its rearrangement gives access to very diverse isomers and addition products with comparable relative energies and reaction barriers. The results are compared to our previous study on the analogous osmium system OsO_3CH_2 and we show that reactivity of both compounds towards ethylene is quite similar. In both cases, the $[3+2]_{C,O}$ cycloaddition pathway is preferred kinetically and thermodynamically. The exothermicity (−68.8 kcal/mol) of this reaction is higher for the ruthenium system than for the osmium homologue. While this pathway is unrivaled for the osmium system, the $[3+2]_{O,O}$ cycloaddition pathway is able to compete kinetically for the ruthenium system.

© 2008 Elsevier B.V. All rights reserved.

1. Introduction

The use of OsO_4 as catalyst for *cis*-dihydroxylation of olefins has become a standard procedure in organic chemistry [1]. After some debate about the nature of the initial addition step, quantum chemical studies clearly revealed that it is a concerted [3 + 2] addition process yielding an osma-2,5-dioxolane. The alternatively suggested route (i.e., [2 + 2] addition followed by subsequent rearrangement of the osmaoxetane) was shown to have much higher activation barriers [2]. For RuO_4, a similar reaction mechanism was proposed [3] and the [3 + 2] initial step is supported by recent experiments [4]. While these findings are now undisputed in the community, much less is known about the reactivity of ethylene with transition metal compounds containing doubly bonded ligands (=X) other than oxygen. In this context we note that Deubel and Muñiz reported a theoretical study of the ethylene addition to $OsO_2(NH)_2$ and clearly showed that again [3 + 2] addition dominates over [2 + 2] addition pathways [5].

However, a considerably different picture arose in our recent theoretical studies on the corresponding reactivity of the related carbene species $OsO_3(CH_2)$ [6], $OsO_2(CH_2)_2$ [7], $ReO_2(CH_2)(CH_3)$ [8], as well as $WO(CH_2)(CH_3)_2$ [9], and the other group-6 analogs [10] with ethylene. For some of these systems, the [2 + 2] addition of ethylene becomes competitive or even more favorable than the [3 + 2] addition reaction. Further, compared to the binary metal oxides, substantially more complicated reaction profiles were identified in these studies, because C–C and C–O ring closure reactions can lead to a number of thermodynamically favorable intermediates that open up further reaction pathways. Interestingly, Schrock has recently reported the synthesis of RR′W(NAr)($CHCMe_3$) and its reaction with ethylene yielding RR′W(NAr)(CH_2) and $H_2C{=}CHCMe_3$, which indicates that a [2 + 2] addition across the $W{=}CHCMe_3$ double bond has taken place [11].

As part of our ongoing studies of ethylene addition to such species we present here results of quantum chemical calculations on the ethylene addition to $RuO_3(CH_2)$, the Ru homologue of $OsO_3(CH_2)$ studied earlier [8]. A comparison of the reaction pathways identified for these two systems is made in order to illustrate similarities and differences caused by variation of the transition metal ion within an identical ligand environment.

2. Computational details

All calculations have been performed at the density functional theory (DFT) level employing the B3LYP hybrid functional [12] as implemented [13] in the GAUSSIAN03 program [14]. The TZVP all electron basis set of Ahlrichs and coworkers was employed for C, O, and H [15]. For Ru the Stuttgart/Köln relativistic effective core potentials replacing 28 core electrons were used in combination with (311111/22111/411) valence basis sets [16]. This combination is denoted here as basis set I. All minima and transition structures were optimized at this level of theory without symmetry constraints. Analytic Hessians computed at B3LYP/I were used to characterize the nature of stationary points as local minima or transition states and to obtain (unscaled) zero-point vibrational energy contributions (ZPE). All connectivities of minima and

* Corresponding authors.
E-mail addresses: Frenking@chemie.uni-marburg.de (G. Frenking), Max.Holthausen@chemie.uni-frankfurt.de (M.C. Holthausen).

0022-328X/$ - see front matter © 2008 Elsevier B.V. All rights reserved.
doi:10.1016/j.jorganchem.2008.10.017

transition structures were verified by either intrinsic reaction coordinate (IRC) [17] or dynamic reaction path (DRP) [18] following calculations with a slightly different valence basis set for Ru. Here, the triple-ζ quality valence basis set (31111/411/311) was used [19]. Based on the B3LYP/I geometries additional single point calculations were performed employing the larger basis set II, in which the Stuttgart/Köln valence basis set for Ru was augmented by two sets of *f*-functions and one set of *g*-functions derived by Martin and Sundermann [20] and used in combination with the correlation consistent cc-pVTZ basis set of Dunning [21] for C, O, and H atoms. All relative energies discussed below relate to B3LYP/II/B3LYP/I calculations and include ZPE contributions. While the B3LYP functional used together with basis sets of triple-ζ quality can show errors in computed barrier heights as large as 4–7 kcal/mol [22] we found by comparison to CCSD(T)/II calibration data in earlier work [7] relative energies obtained at the B3LYP/II//B3LYP/I level superior to relative energies directly obtained from B3LYP/I calculations. Our present results are consistent and directly comparable with our previously published data in [6], but please note that a different basis set was used in our first report [8] on the reactivity of $OsO_3(CH_2)$ against ethylene.

3. Results and discussion

The focus of this work lies on the calculated reaction profiles for the addition of ethylene to RuO_3CH_2 (^{Ru}**1**) and the comparison to those predicted earlier for OsO_3CH_2 (^{Os}**1**). We refrain from a detailed discussion of molecular structures, but a complete set of coordinates and total energies (B3LYP/I and B3LYP/II//B3LYP/I) of all ruthenium species discussed is given as Supporting Information.

In our previous studies on ethylene addition to alkylidene species $L_nM(CH_2)(O)$, we found that the parent complex may rearrange to more stable isomers [6–9]. We thus commenced our study with a search for conceivable isomers of RuO_3CH_2 (**1**) and the associated transition structures. The results are shown in Fig. 1.

Indeed, we found that, with the two exceptions **1c** and **1e** (26.6 and 31.3 kcal/mol relative to **1**, respectively), all identified isomers are more stable than **1**. Notably, the ruthenaoxirane isomer **1a** is substantially more stable than **1** by 51.2 kcal/mol. The O–C coupling step proceeds via **TS1→1a** and is connected with a barrier of 28.6 kcal/mol. The resulting species can then rearrange to **1d** which can be interpreted as the end-on complex of formaldehyde and RuO_2. The barrier involved in this process is moderate

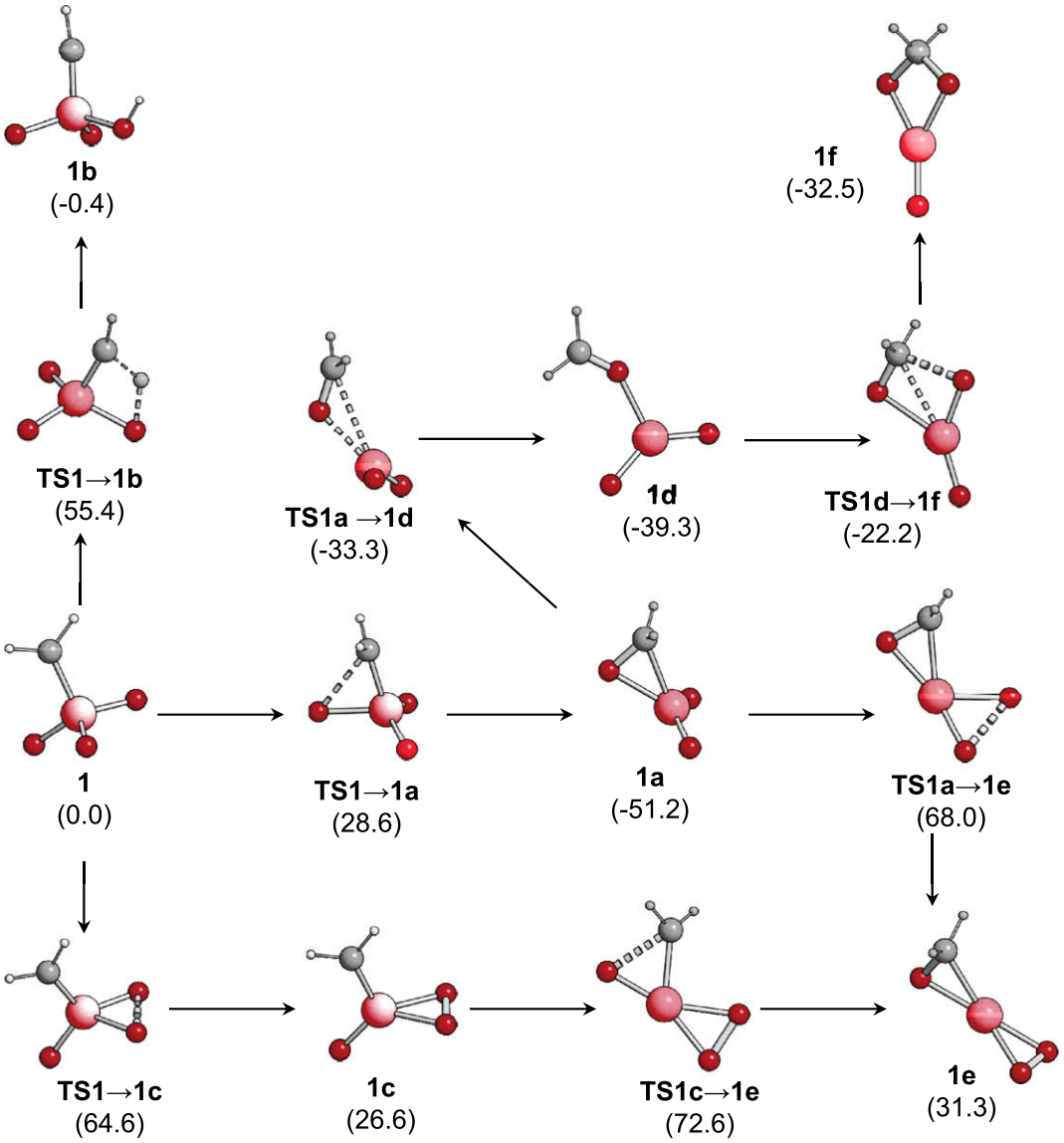

Fig. 1. Isomerization pathways of **1** (energies in kcal/mol relative to **1** + C_2H_4).

(−33.0 kcal/mol relative to **1**, barrier height 18.2 kcal/mol). Further rearrangement leads to the symmetrically O–CH_2–O bridged **1f**, which is still more stable than **1** (−32.5 kal/mol), but significantly less stable than **1a**. Another isomerization process involves H-migration via **TS1→1b** to form **1b**, which is only slightly more stable than **1** (by 0.4 kcal/mol). Yet, the high barrier for its formation (55.4 kcal/mol) renders this process irrelevant in the present context. An even higher barrier (64.6 kcal/mol) is connected with the O–O bond formation via **TS1→1c** leading to formation of the peroxo isomer **1c**, which is significantly less stable than **1** (by 26.6 kcal/mol). The doubly side-on coordinated structure **1e** can then be reached through rearrangement of **1a** (activation barrier 119.2 kcal/mol) or **1c** (activation barrier 46.0 kcal/mol), but is significantly less stable than **1** and connected with high activation barriers. These findings suggest that **1** actually represents a rather unstable isomer. Due to high activation barriers connected to most of its isomers, however, the only potentially relevant isomerization process to be considered in the following is formation of **1a**, the other pathways are kinetically strongly disfavored.

Next, we investigated the addition pathways of ethylene to **1**. The computed reaction profiles are illustrated in Fig. 2.

We found three direct pathways for the ethylene addition to **1**. A [3 + 2] addition to the O=Ru=O group occurs via **TS1→2** almost barrierless and yields the methyleneoxoruthena-2,5-dioxolane **2**. This process is strongly exothermic by 44.2 kcal/mol. An even stronger thermodynamic driving force of 68.8 kcal/mol is found for the [3 + 2] addition of ethylene to the O=Ru=CH_2 group to form the dioxoruthena-2-oxolane **3**. Also this process occurs without barrier [23]. As a third pathway we identified the addition of ethylene to one of the oxygen atoms with concomitant hydrogen migration from ethylene to the carbene group in **1** that occurs via **TS1→4**. The resulting species **4** is 56.3 kcal/mol more stable than **1** + C_2H_4, but with an activation barrier of 16.2 kcal/mol this process is kinetically significantly disfavored compared to the [3 + 2] addition pathways. A similar process is the reaction of **1** to **4a** through **TS1→4a**. Here, a hydrogen migrates from the ethylene to an oxo group, while the C_2-fragment adds to the carbene moiety. This reaction is exothermic by 62.9 kcal/mol, but with a

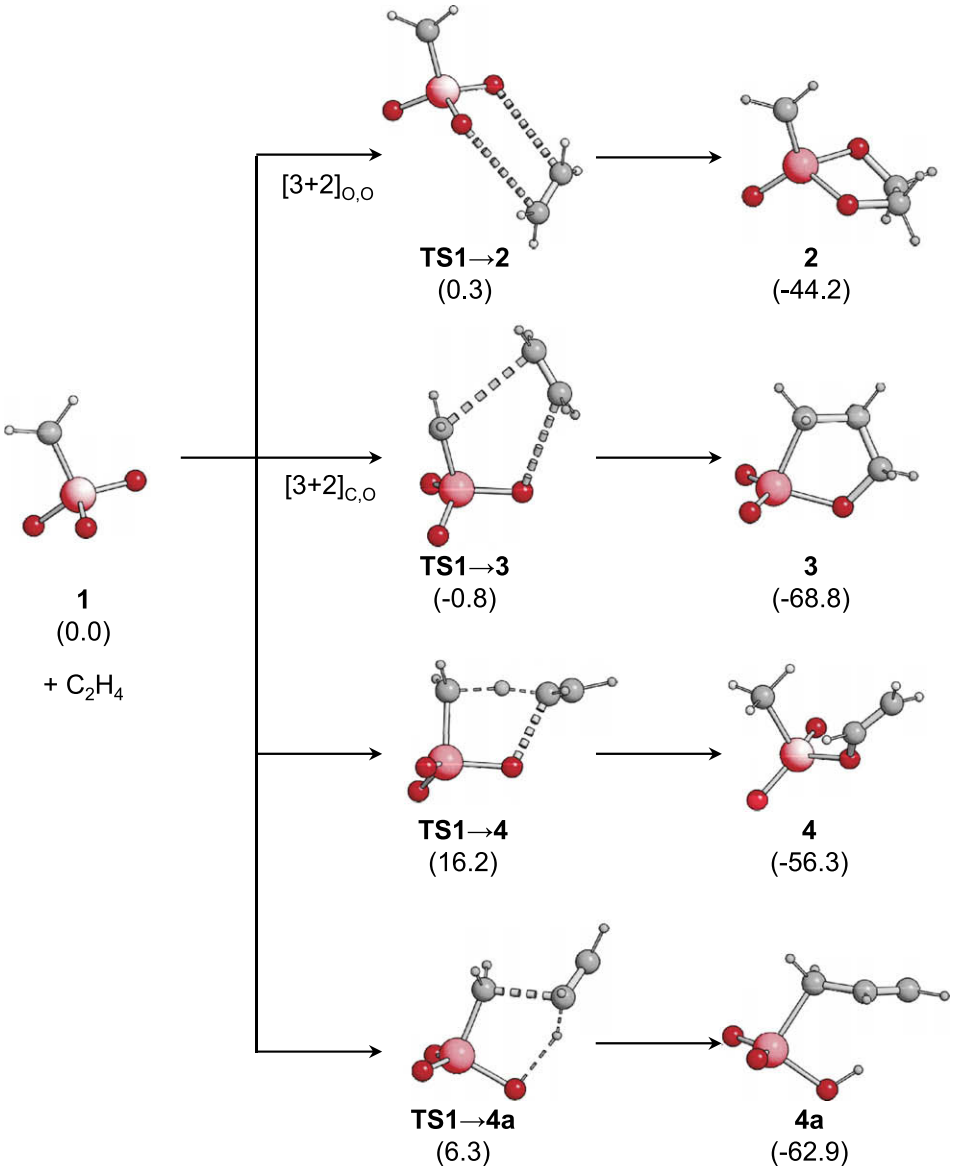

Fig. 2. Reaction pathways for the addition of ethylene to **1** (energies in kcal/mol relative to **1** + C_2H_4).

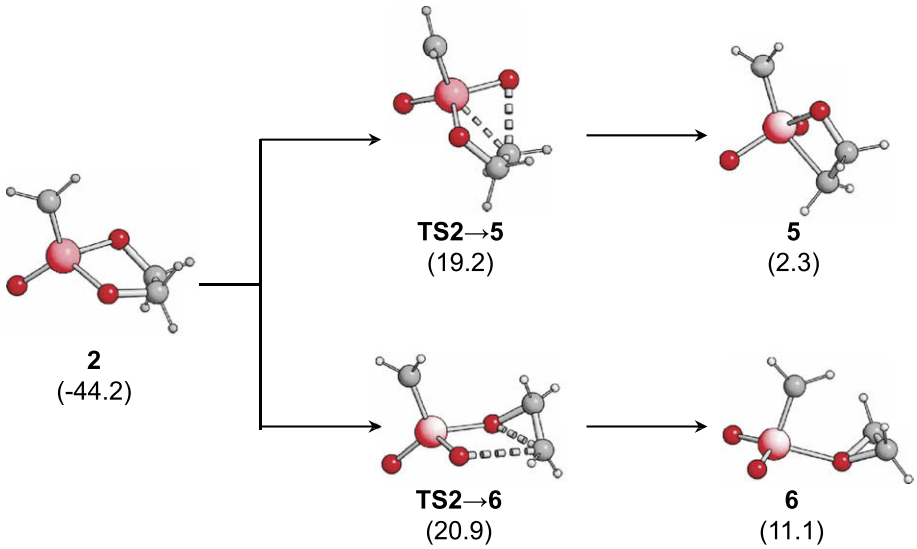

Fig. 3. Reaction pathways for the rearrangement of **2** (energies in kcal/mol relative to **1** + C_2H_4).

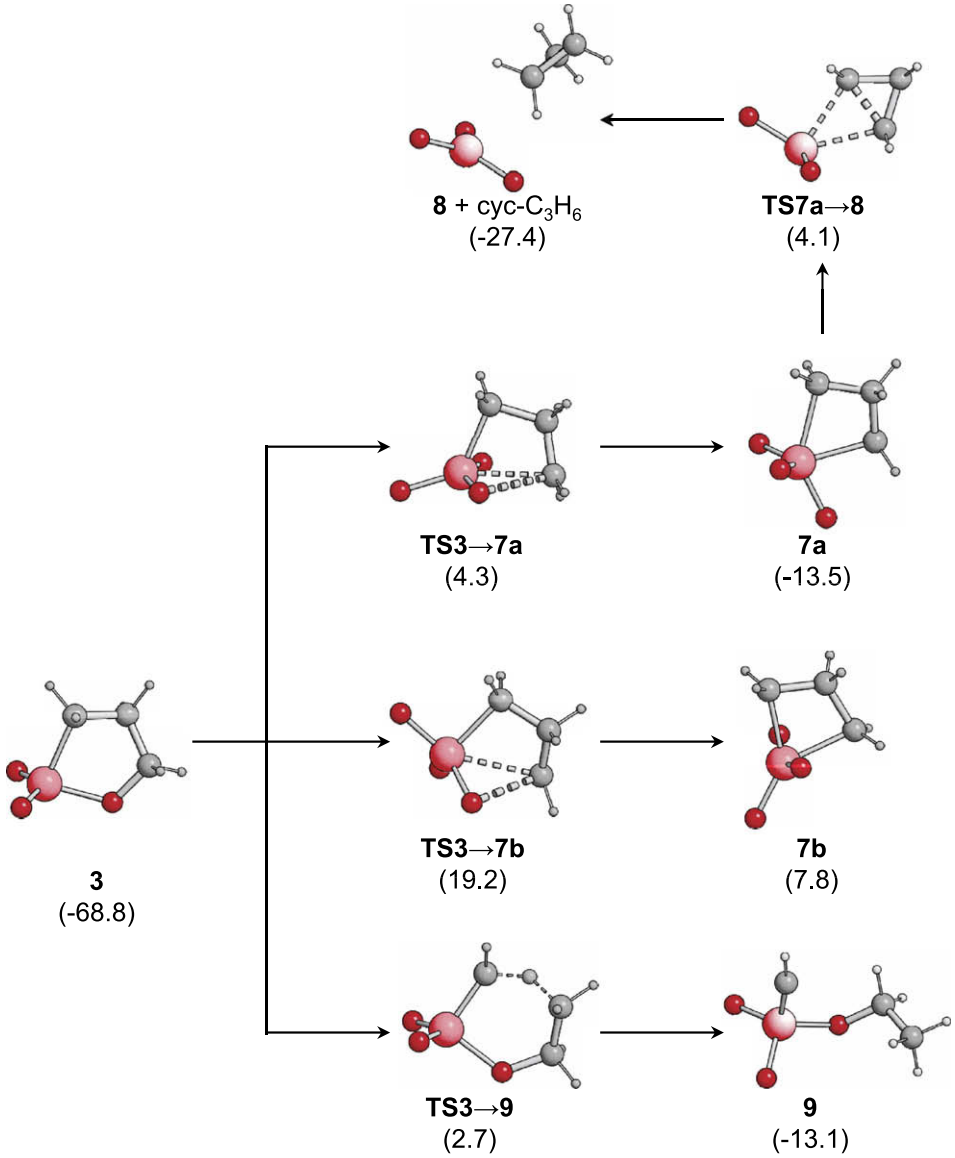

Fig. 4. Reaction pathways for the rearrangement of **3** (energies in kcal/mol relative to **1** + C_2H_4).

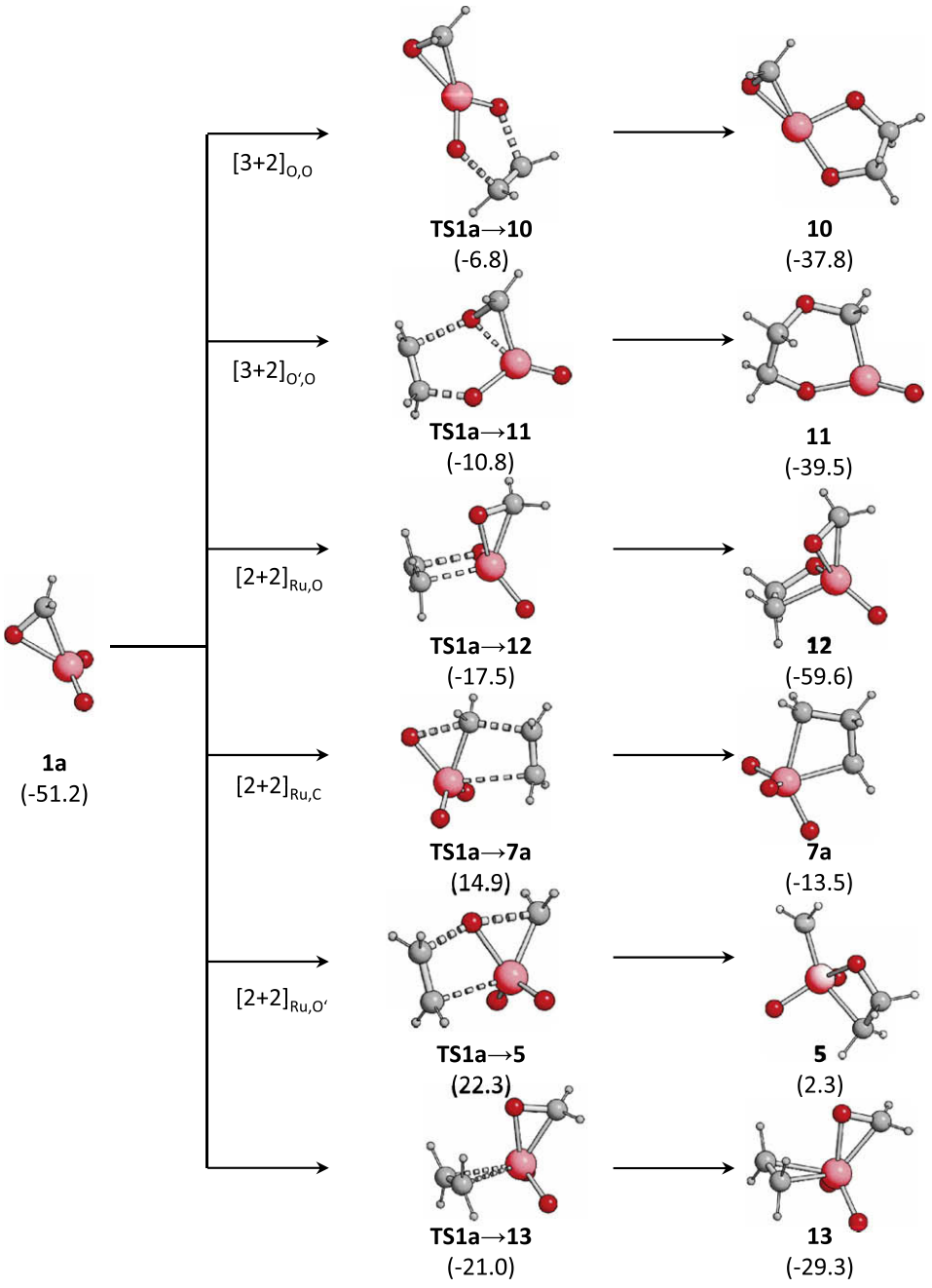

Fig. 5. Reaction pathways for addition of ethylene to **1a** (energies in kcal/mol relative to **1** + C_2H_4).

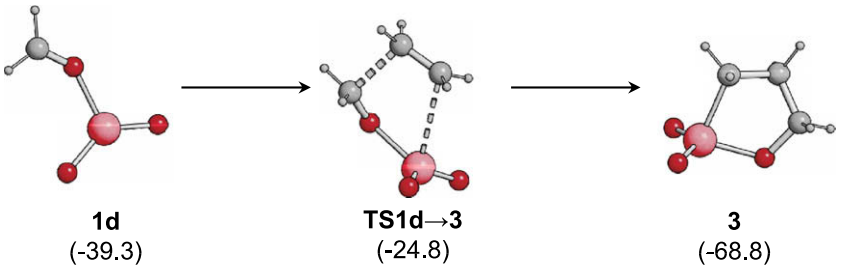

Fig. 6. Lowest energy pathway for addition of ethylene to **1d** (energies in kcal/mol relative to **1** + C_2H_4).

barrier of 6.3 kcal/mol this process is kinetically disfavored as compared to [3 + 2] addition pathways. We did not find any further reaction pathways for the addition of ethylene to **1**, and in particular we were unable to identify any direct [2 + 2] addition process.

Two of the four products formed in these initial steps can undergo further rearrangements (Figs. 3 and 4). Isomer **5** is only slightly less stable than **1** + C_2H_4 by 2.3 kcal/mol and can be viewed as formal product of a [2 + 2] cycloaddition of ethylene across the Ru=O double bond. Via **TS2→5** this step is connected with an activation barrier of 19.2 kcal/mol relative to **1** + C_2H_4. Alternatively, a complex between $RuO_2(CH_2)$ and ethylene oxide, **6** (11.1 kcal/mol less stable than **1**) can be formed from **2** in a concerted step via **TS2→6**, with an activation barrier of 20.9 kcal/mol relative to **1** + C_2H_4. As both pathways start from intermediate **2**, which is 44.2 kcal/mol more stable than **1** + C_2H_4, the ring contraction as well as the epoxide formation constitute strongly endothermic processes with excessively large activation barriers, which both are hence irrelevant in the overall reaction.

Along the subsequent isomerization pathways studied for **3** (Fig. 4), we localized two isomers **7a** and **7b** that can be viewed as the formal products of a [2 + 2] cycloaddition of ethylene across the Ru=CH_2 double bond. The former species is 13.5 kcal/mol more stable than **1** + C_2H_4 whereas the latter is less stable by 7.8 kcal/mol. Both ring contractions are connected with the two transition states **TS3→7a** and **TS3→7b** that lie 4.3 and 19.2 kcal/mol higher in energy than **1** + C_2H_4, respectively. Once **7a** is formed, subsequent elimination of cyclopropane can take place via **TS7a→8**, which lies only 4.1 kcal/mol above **1** + C_2H_4. We identified yet another reaction path that results in the formation of **9** (13.1 kcal/mol more stable than **1** + C_2H_4) after passage of the rather low lying **TS3→9** (2.7 kcal/mol above **1** + C_2H_4), the transition state of a ring opening in **3** by C–C cleavage with concomitant hydrogen migration.

Taken together we identified five reaction channels for the decay of intermediates **2** and **3**, and two of these routes result in species that are more stable than **1** + C_2H_4, with low lying transition structures on the same energy scale. They all start, however, from very stable intermediates (**2**: −44.2 kcal/mol, **3**: −68.8 kcal/mol relative to **1** + C_2H_4). Thus, these routes are in fact connected with prohibitively high activation barriers and represent strongly endothermic processes. All in all we conclude that all of these processes are unlikely to take place in the overall course of the reaction and also the initial isomerization to the rather stable species **1a** cannot compete with the barrierless [3 + 2] ethylene additions yielding **2** and **3** as thermodynamically and kinetically preferred products.

As noted above, a modest barrier height (28.6 kcal/mol) together with the strong exothermicity found for the formation of **1a** (−51.2 kcal/mol relative to **1**) renders this species relevant in potential attempts to synthesize **1** or derivatives thereof. Therefore, we also investigated initial reaction steps starting from **1a** (Fig. 5).

We identified six individual reaction channels for the addition of ethylene to **1a**. Two of them can be classified as [3 + 2] cycloadditions, whereas only **TS1a→10** results in formation of a five-membered ring, **10**. **TS1a→11** results in a six-membered ring **11** due to scission of the C–O and O–Ru bonds. Both addition products are more stable than **1** + C_2H_4 by −37.8 and −39.5 kcal/mol, respectively, but with respect to **1a**, both reactions are endothermic and are connected with high barriers exceeding 40 kcal/mol.

While no [2 + 2] cycloaddition pathways could be identified for **1**, there are three such routes for **1a**. The formal products of [2 + 2] cycloaddition to **1** are accessible through **TS1a→5** and **TS1a→7a** by C–O bond cleavage in the course of the reaction. Yet, with 73.5 and 66.1 kcal/mol the corresponding reaction barriers are prohibitively high. Interestingly, the reaction barrier **TS1a→12** is lower than the identified [3 + 2] addition pathways. This is in contrast to the other investigated isomers of **1**, where [3 + 2] addition is consistently preferred over [2 + 2] addition.

The last reaction channel identified for addition to **1a** is direct addition of ethylene, forming the ruthenacyclopropane **13**. **TS1a→13** possesses the lowest barrier identified so far for the ethylene addition to **1a** (30.2 kcal/mol), but **13** is less stable than **1a** + C_2H_4 by 21.9 kcal/mol. Further, recalling the rearrangement reactions from Fig. 1, we find the rearrangement of **1a** to **1d** kinetically favored by 12.3 kcal/mol with respect to the reaction via **TS1a→13**.

From **1d** then, addition of ethylene (Fig. 6) in a [3 + 2] fashion is possible via **TS1d→3** (−24.8 kcal/mol relative to **1** + C_2H_4, activation barrier 14.5 kcal/mol), which represents the most favorable reaction pathway starting from this species (other pathways were identified, but are not presented here).

4. Comparison with the system $OsO_3CH_2 + C_2H_4$

Let us now compare the key reaction steps evolving from our present study on the system $RuO_3(CH_2) + C_2H_4$, with the corresponding pathways studied earlier for the $OsO_3CH_2 + C_2H_4$ system. To facilitate the comparison, we use a common numbering scheme here, and in the following the respective transition metal ion ad-

Table 1
Total energies in a.u. and relative energies in kcal/mol (including zero point energy contributions) for all intermediates and transition states. ZPE contributions were obtained at the B3LYP/I level of theory and are included to obtain E_0 at the B3LYP/II level.

Structure	E_{tot}	ZPE	E_0^{rel}	E_{tot}	E_0^{rel}
	B3LYP/I	B3LYP/I	B3LYP/I	B3LYP/II	B3LYP/II + ZPE
C_2H_4	−78.62155	0.05095		−78.62317	
1	−359.86572	0.03264	0.0	−359.90792	0.0
1a	−359.95613	0.03619	−54.5	−359.99308	−51.2
TS1→1a	−359.82480	0.03233	25.5	−359.86202	28.6
1b	−359.87076	0.03284	−3.2	−359.90879	−0.4
TS1→1b	−359.76898	0.02740	35.0	−359.81437	55.4
1c	−359.83164	0.03267	21.4	−359.86553	26.6
TS1→1c	−359.76904	0.03139	59.9	−359.80374	64.6
1d	−359.93988	0.03504	−45.0	−359.97291	−39.3
TS1a→1d	−359.92778	0.03348	−38.4	−359.96191	−33.3
1e	−359.83659	0.03478	19.6	−359.86026	31.3
TS1a→1e	−359.77437	0.03375	58.0	−359.80062	68.0
TS1c→1e	−359.75947	0.03179	66.1	−359.79136	72.6
1f	−359.92798	0.03742	−36.1	−359.96456	−32.5
TS1d→1f	−359.90952	0.03515	−25.9	−359.94585	−22.2
2	−438.57695	0.09160	−51.2	−438.60961	−44.2
TS1→2	−438.48770	0.08437	−0.3	−438.53141	0.3
3	−438.61474	0.09419	−73.3	−438.65127	−68.8
TS1→3	−438.49013	0.08483	−1.8	−438.53353	−0.8
TS1d→3	−438.54127	0.08936	−30.3	−438.57643	−24.8
4	−438.58940	0.08908	−64.1	−438.62625	−56.3
TS1→4	−438.46426	0.08286	14.4	−438.50457	16.2
4a	−438.60156	0.09098	−71.7	−438.63863	−62.9
TS1→4a	−438.48342	0.08651	2.4	−438.52385	6.3
5	−438.49780	0.08964	−2.8	−438.53353	2.3
TS1a→5	−438.45808	0.08638	20.1	−438.49841	22.3
TS2→5	−438.47044	0.08839	13.6	−438.50536	19.2
6	−438.48785	0.08950	−0.4	−438.51933	11.1
TS2→6	−438.46890	0.08712	11.5	−438.50127	20.9
7a	−438.51878	0.09142	−14.9	−438.56036	−13.5
TS1a→7a	−438.47113	0.08799	12.9	−438.51175	14.9
TS3→7a	−438.48864	0.08959	3.6	−438.53031	4.3
7b	−438.48317	0.09211	2.6	−438.52720	7.8
TS3→7b	−438.46638	0.08956	13.1	−438.50644	19.2
8	−438.53771	0.08940	−31.7	−438.58058	−27.4
TS7a→8	−438.49207	0.09030	−3.0	−438.53130	4.1
9	−438.51815	0.08922	−19.4	−438.55765	−13.1
TS3→9	−438.49213	0.08665	−3.0	−438.52986	2.7
10	−438.57795	0.09413	−50.3	−438.60181	−37.8
TS1a→10	−438.52111	0.08952	−17.5	−438.54786	−6.8
11	−438.57806	0.09593	−49.2	−438.60639	−39.5
TS1a→11	−438.52314	0.08987	−18.6	−438.55473	−10.8
12	−438.60184	0.09264	−66.2	−438.63520	−59.6
TS1a→12	−438.53346	0.08981	−25.1	−438.56515	−17.5
13	−438.55236	0.09080	−36.3	−438.58503	−29.3
TS1a→13	−438.53729	0.08886	−28.1	−438.56992	−21.0

dressed is denoted by a preceding element symbol as superscript. Total and relative energies at the different levels of theory are presented in Table 1.

Figs. 7 and 8 show reaction pathways for ethylene addition to the carbene species $^{Ru/Os}$**1.** In contrast to our study on the osmium system, we found no transition states directly connecting ^{Ru}**1** with

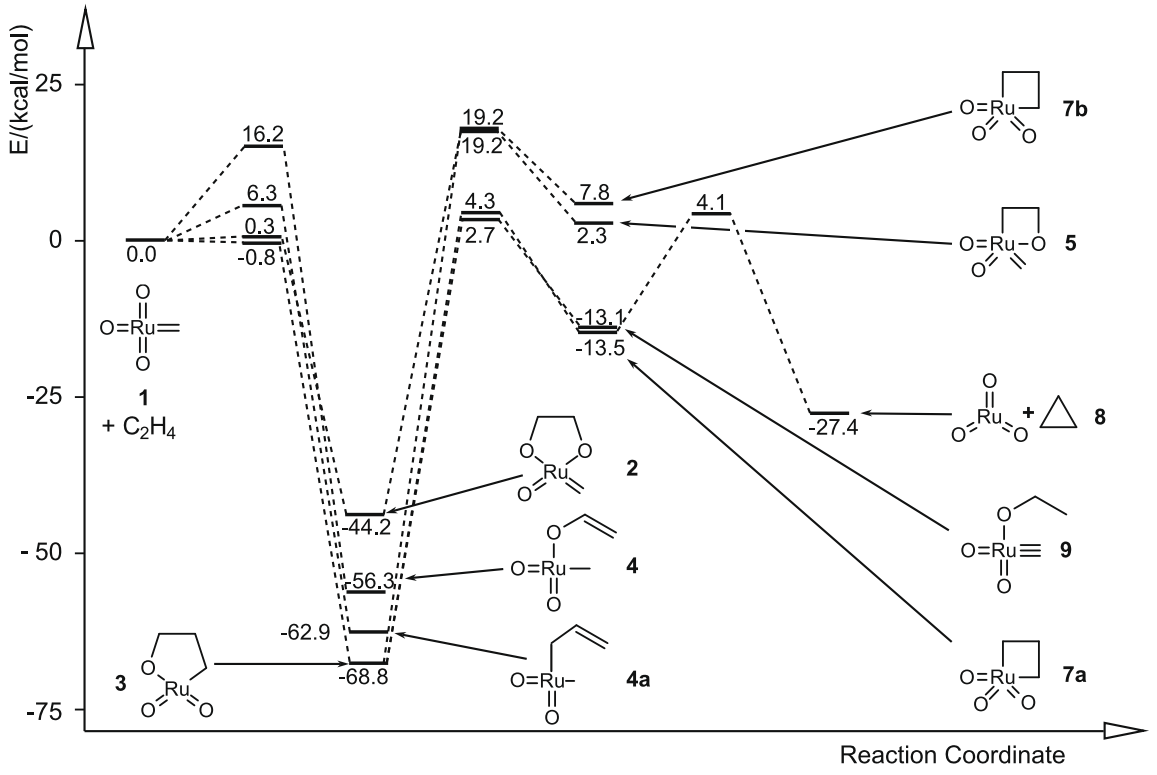

Fig. 7. Computed reaction profile for the addition of ethylene to $RuO_3(CH_2)$ (energies in kcal/mol relative to ^{Ru}**1** + C_2H_4).

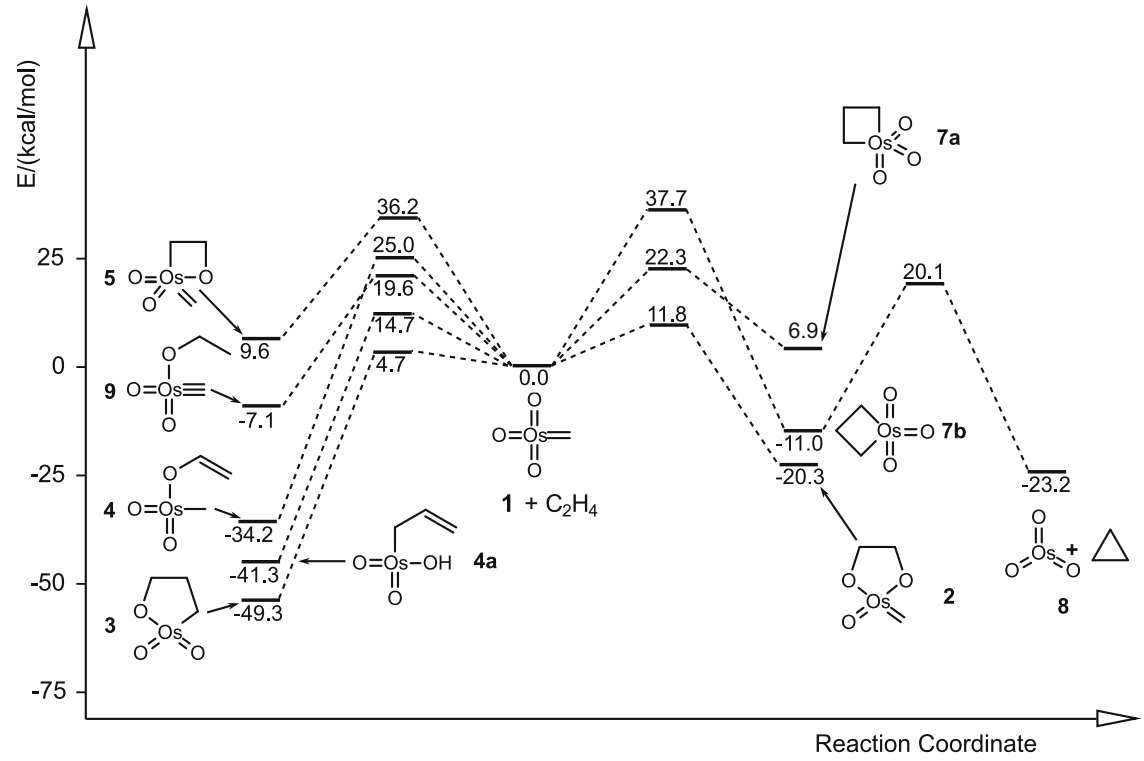

Fig. 8. Computed reaction profile for the addition of ethylene to $OsO_3(CH_2)$ (energies in kcal/mol relative to ^{Os}**1** + C_2H_4).

one of the addition products ^{Ru}**5**, ^{Ru}**7a**, ^{Ru}**7b**, or ^{Ru}**9**; these species are formed instead by isomerizations of the primary intermediates ^{Ru}**2** and ^{Ru}**3**. These interconversion routes cannot compete, neither energetically nor kinetically, with the cycloaddition products ^{Ru}**2**

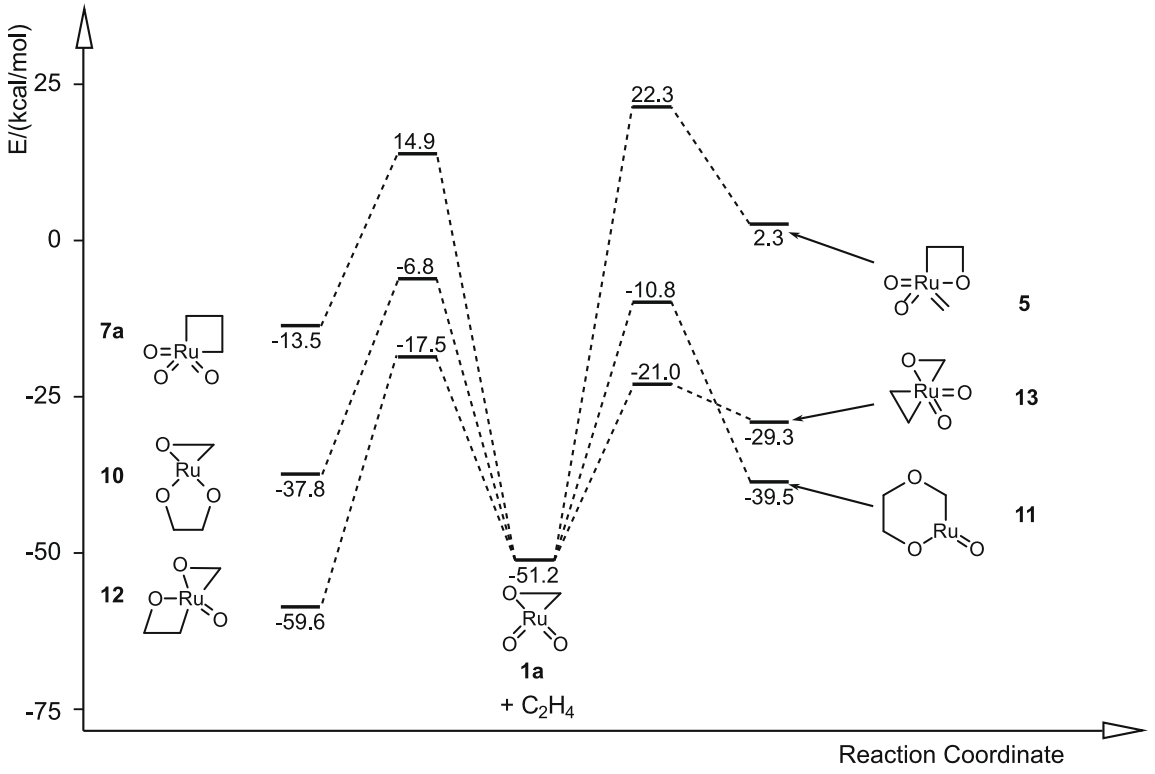

Fig. 9. Computed reaction profile for the addition of ethylene to ^{Ru}**1a** (energies in kcal/mol relative to ^{Ru}**1** + C_2H_4).

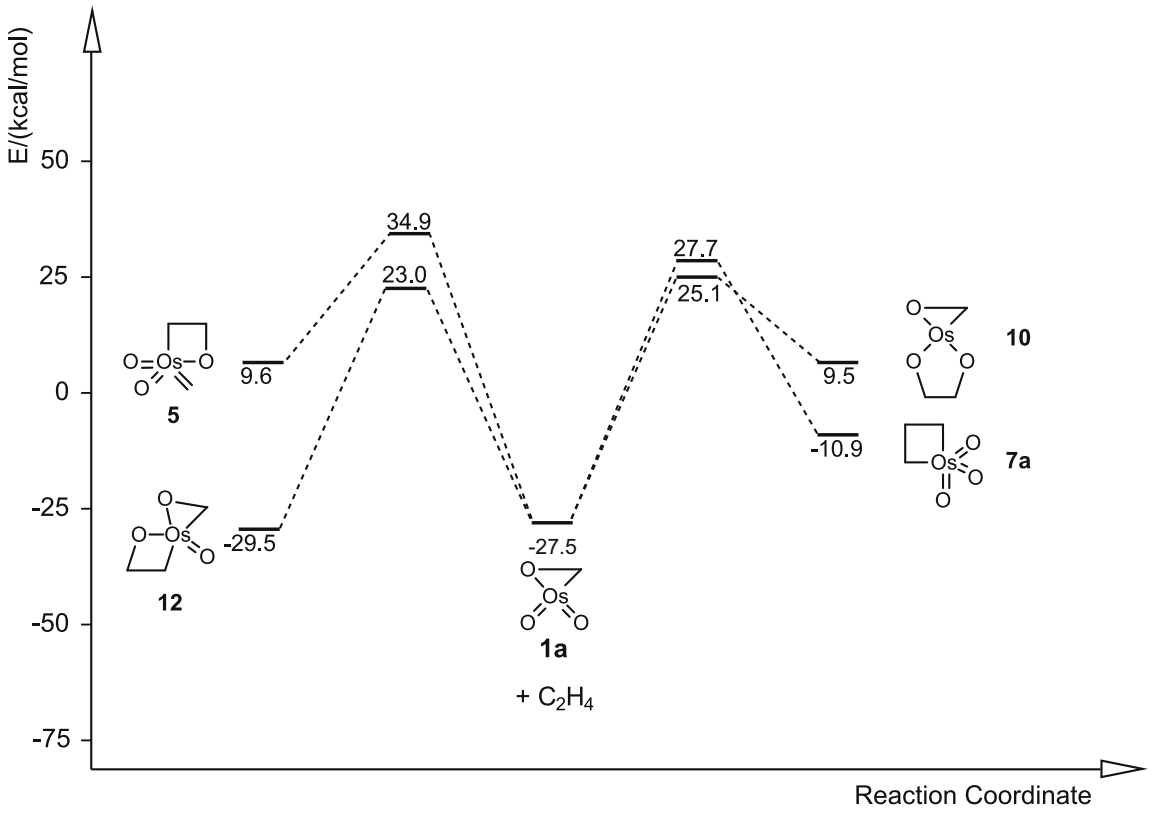

Fig. 10. Computed reaction profile for the addition of ethylene to ^{Os}**1a** (energies in kcal/mol relative to ^{Os}**1** + C_2H_4).

and ^{Ru}**3** formed in a single step directly from ^{Ru}**1**. Also for the Os system formation of ^{Os}**2** and ^{Os}**3** is kinetically and thermodynamically preferred over formation of the corresponding species ^{Os}**5**, ^{Os}**7a**, ^{Os}**7b** and ^{Os}**9**, although the predominance of the former pathways is much less pronounced than in the Ru system. Here, the high stability of intermediates ^{Ru}**2** and ^{Ru}**3** causes prohibitively large barriers for the subsequent steps.

For ^{Ru}**1** and ^{Os}**1**, the most favorable [3 + 2] cycloaddition pathways occur via $^{Ru/Os}$**TS1**→**2** and $^{Ru/Os}$**TS1**→**3**. We consistently find the $[3+2]_{C,O}$ addition pathway preferred over the $[3+2]_{O,O}$ route for both systems. Presumably, the very low lying transition states for [3 + 2] additions in ^{Ru}**1** preclude identification of any genuine first-order saddle-points for [2 + 2] additions to the Ru–O and Ru–C bond, respectively. All our attempts to identify such structures repeatedly resulted either in transition states for [3 + 2] addition or in higher order saddle points, with at least one additional imaginary mode associated with the reorientation towards the [3 + 2] transition state or its products.

For both metal ions, formation of side-on peroxo ligated species is strongly disfavored, kinetically as well as thermodynamically (cf. Fig. 1). For both systems, however, rearrangement of $^{Ru/Os}$**1** yields metallaoxirane species $^{Ru/Os}$**1a** that are substantially more stable than the parent carbene species. A significant difference is found for the relative energies of ^{Ru}**1a** (51.2 kcal/mol below ^{Ru}**1**) and for the corresponding barrier ^{Ru}**TS1**→**1a** (28.6 kcal/mol) as compared to the **Os** system (−33.3 and +36.6 kcal/mol, respectively). Ethylene addition to these intermediates gives rise to several additional reaction pathways that are shown in Fig. 9 (Ru system) and Fig. 10 (Os system).

For the ruthenium system, four barriers are located below the relative energy of ^{Ru}**1**, which under gas phase conditions should open additional reaction pathways commencing from ^{Ru}**1a** to form ^{Ru}**10**, ^{Ru}**11**, ^{Ru}**12**, and ^{Ru}**13** that are not accessible for ^{Os}**1a**. Under condensed phase conditions, however, all ethylene addition processes starting from $^{Ru/Os}$**1a** would be connected with higher barriers for the Ru system compared to the Os system.

And finally, we identified an unexpected reaction pathway for the Ru system, which is not accessible for the Os system: Isomerization of ^{Ru}**1a** to ^{Ru}**1d** via ^{Ru}**TS1a**→**1d** is connected with a moderately low barrier of about 18 kcal/mol relative to ^{Ru}**1a** and subsequent ethylene addition to ^{Ru}**1d** via ^{Ru}**TS1d**→**3** yields ^{Ru}**3** with an even lower barrier (about 15 kcal/mol relative to ^{Ru}**1d**). Connected by two moderately high barriers this additional reaction path leads to the same product as does the most favorable direct addition pathway of ethylene to ^{Ru}**1**. Hence, since ^{Ru}**TS1**→**2** and ^{Ru}**TS1**→**3** are found to be kinetically competitive, ^{Ru}**2** and ^{Ru}**3** should be formed in appreciable amounts, while the corresponding Os-system should preferably form ^{Os}**3**.

A closer comparison of all transition states and intermediates in this investigation reveals that all structures containing Ru in a lowered formal oxidation state are stabilized compared to the corresponding species containing Os ions. This fits well with the general rule that higher oxidation states of homologs are more stable the heavier the central element. The reactivity presented herein is thus mostly driven by formal Ru^{VI} chemistry, whereas the results presented earlier for Os reflect the strong preference for Os^{VIII} chemistry.

5. Summary

The calculated reaction pathways for the ethylene addition to RuO_3CH_2 (^{Ru}**1**) and OsO_3CH_2 (^{Os}**1**) exhibit only minor qualitative differences. For both systems, the $[3+2]_{C,O}$ cycloaddition pathway is preferred thermodynamically and kinetically with a large exothermicity (−68.8 kcal/mol for M = Ru, −49.3 kcal/mol for M = Os) and negligible barriers. For M = Ru, the $[3+2]_{O,O}$ cycloaddition pathway is significantly less exothermic, but it can in fact compete kinetically with the $[3+2]_{C,O}$ route because it also occurs nearly barrierless (for M = Os, the corresponding barrier is 10.5 kcal/mol higher). The present results indicate that isomerizations of ^{M}**1** prior to the ethylene addition step do not alter the product distribution for both metals. While for ^{Os}**1**, these isomerization reactions are found to be kinetically hindered, ^{Ru}**1** is found to be thermodynamically unstable toward decay to ^{Ru}**1a**. This isomerization reaction is also kinetically accessible. Somewhat surprisingly, we find that such isomerization should not alter the overall mechanistic picture for the reaction of ^{Ru}**1** with ethylene, because ethylene addition to the isomerized ^{Ru}**1a** results in formation of the identical product (^{Ru}**3**).

Acknowledgments

This work was supported by the Deutsche Forschungsgemeinschaft. The generous allotment of computer time by the HRZ Marburg, the CSC Frankfurt, the HHLR Darmstadt, as well as their excellent service is gratefully acknowledged.

Appendix A. Supplementary material

Supplementary data associated with this article can be found, in the online version, at doi:10.1016/j.jorganchem.2008.10.017.

References

[1] M. Schröder, Chem. Rev. 80 (1980) 187.
[2] (a) D.V. Deubel, G. Frenking, Acc. Chem. Res. 36 (2003) 645;
(b) U. Pidun, C. Boehme, G. Frenking, Angew. Chem. 108 (1996) 3008;
U. Pidun, C. Boehme, G. Frenking, Angew. Chem., Int. Ed. Engl. 35 (1996) 2817;
(c) S. Dapprich, G. Ujaque, F. Maseras, A. Lledós, D.G. Musaev, K. Morokuma, J. Am. Chem. Soc. 118 (1996) 11660;
(d) A.M. Torrent, L. Deng, M. Duran, M. Sola, T. Ziegler, Organometallics 16 (1997) 13;
(e) A.J. Del Monte, J. Haller, K.N. Houk, K.B. Sharpless, D.A. Singleton, T. Straßner, A.A. Thomas, J. Am. Chem. Soc. 119 (1997) 9907.
[3] (a) J. Frunzke, C. Loschen, G. Frenking, J. Am. Chem. Soc. 126 (2004) 3642;
(b) T. Strassner, M. Drees, Theochem 671 (2004) 197;
(c) P.-O. Norrby, H.C. Kolb, K.B. Sharpless, Organometallics 13 (1994) 344.
[4] (a) W.-P. Yip, W.-Y. Yu, N. Zhu, C.-M. Che, J. Am. Chem. Soc. 127 (2005) 14239;
(b) B. Plietker, M. Niggemann, A. Pollrich, Org. Biomol. Chem. 2 (2004) 1116;
(c) B. Plietker, M. Niggemann, Org. Lett. 5 (2003) 3353.
[5] D.V. Deubel, K. Muñiz, Chem. Eur. J. 10 (2004) 2475.
[6] R. Haunschild, C. Loschen, S. Tüllmann, D. Cappel, M. Hölscher, M.C. Holthausen, G. Frenking, J. Phys. Org. Chem. 20 (2007) 11.
[7] M. Hölscher, W. Leitner, M.C. Holthausen, G. Frenking, Chem. Eur. J. 11 (2005) 4700.
[8] D. Cappel, S. Tüllmann, C. Loschen, M.C. Holthausen, G. Frenking, J. Organomet. Chem. 691 (2006) 4467.
[9] R. Haunschild, G. Frenking, Z. Naturforsch. B 62 (2007) 367.
[10] R. Haunschild, G. Frenking, J. Organomet. Chem. 693 (2008) 737.
[11] T. Kreickmann, S. Arndt, R.R. Schrock, P. Müller, Organometallics 26 (2007) 5702.
[12] (a) A.D. Becke, J. Chem. Phys. 98 (1993) 5648;
(b) A.D. Becke, Phys. Rev. A 38 (1988) 3098;
(c) C. Lee, W. Yang, R.G. Parr, Phys. Rev. B 37 (1988) 785.
[13] P.J. Stephens, F.J. Devlin, G. Chabalowski, M.J. Frisch, J. Phys. Chem. 98 (1994) 11623.
[14] M.J. Frisch, G.W. Trucks, H.B. Schlegel, G.E. Scuseria, M.A. Robb, J.R. Cheeseman, J.A. Montgomery Jr., T. Vreven, K.N. Kudin, J.C. Burant, J.M. Millam, S.S. Iyengar, J. Tomasi, V. Barone, B. Mennucci, M. Cossi, G. Scalmani, N. Rega, G.A. Petersson, H. Nakatsuji, M. Hada, M. Ehara, K. Toyota, R. Fukuda, J. Hasegawa, M. Ishida, T. Nakajima, Y. Honda, O. Kitao, H. Nakai, M. Klene, X. Li, J.E. Knox, H.P. Hratchian, J.B. Cross, V. Bakken, C. Adamo, J. Jaramillo, R. Gomperts, R.E. Stratmann, O. Yazyev, A.J. Austin, R. Cammi, C. Pomelli, J.W. Ochterski, P.Y. Ayala, K. Morokuma, G.A. Voth, P. Salvador, J.J. Dannenberg, V.G. Zakrzewski, S. Dapprich, A.D. Daniels, M.C. Strain, O. Farkas, D.K. Malick, A.D. Rabuck, K. Raghavachari, J.B. Foresman, J.V. Ortiz, Q. Cui, A.G. Baboul, S. Clifford, J. Cioslowski, B.B. Stefanov, G. Liu, A. Liashenko, P. Piskorz, I. Komaromi, R.L. Martin, D.J. Fox, T. Keith, M.A. Al-Laham, C.Y. Peng, A. Nanayakkara, M. Challacombe, P.M.W. Gill, B. Johnson, W. Chen, M.W. Wong, C. Gonzalez, J.A. Pople, Gaussian 03, Revision D.01, Gaussian, Inc., Wallingford CT, 2004.
[15] A. Schäfer, C. Huber, R. Ahlrichs, J. Chem. Phys. 100 (1994) 5829.

[16] D. Andrae, U. Haeussermann, M. Dolg, H. Stoll, H. Preuss, Theor. Chim. Acta 77 (1990) 123.
[17] (a) K. Fukui, J. Phys. Chem. 74 (1970) 4161;
(b) K. Fukui, Acc. Chem. Res. 14 (1981) 363.
[18] (a) J. Keck, J. Discuss. Faraday Soc. 33 (1962) 173;
(b) J.J.P. Stewart, L. P Davis, L.W. Burggraf, J. Comp. Chem. 8 (1987) 1117;
(c) P.E. Blöchl, H.M. Senn, A. Togni, Molecular reaction modeling from ab initio molecular dynamics, in: D.G. Truhlar, K. Morokuma (Eds.), Transition state modeling for catalysis, ACS Symposium Series, vol. 721, American Chemical Society, Washington, DC, 1999, pp. 88–99. ISBN-13: 978-0841236103.
[19] K. Eichkorn, F. Weigend, O. Treutler, R. Ahlrichs, Theor. Chem. Acc. 114 (1997) 3408.
[20] J.M.L. Martin, A.J. Sundermann , Chem. Phys. 114 (2001) 3408.
[21] T.H. Dunning, J. Chem. Phys. 90 (1989) 1007.
[22] S.S. Yi, E.L. Reichert, M.C. Holthausen, W. Koch, J.C. Weisshaar, Chem. Eur. J. 6 (2000) 2232.
[23] Even though we did not find any significant enthalpic barrier for either pathway, we note that entropic contributions at finite temperatures not considered in our discussion will most likely result in more pronounced barrier heights for the bimolecular processes via **TS1**→**2** and **TS1**→**3**.